Original article

Nutritional and toxic elemental analysis of dry fruits using laser induced breakdown spectroscopy (LIBS) and inductively coupled plasma atomic emission spectrometry (ICP-AES)

I. Rehan [a], M.A. Gondal [b,*], M.A. Almessiere [c], R.A. Dakheel [c,f], K. Rehan [d], S. Sultana [e], M.A. Dastageer [b]

[a] Department of Physics, Islamia College University, Peshawar 25120, Pakistan
[b] Laser Research Group, Physics Department, King Fahd University of Petroleum and Minerals, P.O. Box 5047, Dhahran 31261, Saudi Arabia
[c] Department of Biophysics, Institute for Research and Medical Consultations (IRMC), Imam Abdulrahman Bin Faisal University, Dammam P.O. Box 1982, Saudi Arabia
[d] State Key Laboratory of Magnetic Resonance and Atomic and Molecular Physics, Wuhan Institute of Physics and Mathematics, Innovation Academy of Precision Measurement Science and Technology, Chinese Academy of Sciences, Wuhan 430071, China
[e] Department of Chemistry, Islamia College University, Peshawar 25120, Pakistan
[f] Department of Physics, College of Science, Imam Abdulrahman Bin Faisal University, Dammam P.O. Box 1982, Saudi Arabia

ARTICLE INFO

ABSTRACT

Quantitative investigation of essential and trace heavy elements present in health-beneficial dry fruits (Pistachio, Almonds, Black walnut, White walnut, and Cashew) was investigated using Laser Induced Breakdown Spectroscopy. For an accurate elemental exposure using LIBS technique, the local thermo-dynamical equilibrium of the laser induced plasma was established and verified using McWhirter criterion based on the electron number density in the plasma. Earlier to engage, our LIBS detector was optimized. For quantification of elements, standard calibration curves (CC)-LIBS method was applied. Using our LIBS system, the nutritional elements such as Al, Mg, Ca, Fe, K, Zn, and Na and toxins like Pb, Cr, and Cu were detected in dry fruits. The elemental quantification of dry fruit contents were validated using standard (ICP-AES) method and the relative accuracy of our experimental setup in comparison to ICP approach was in the ranging from 0.1 to 0.3 at 2.5-% error confidence.

1. Introduction

The present study signifies the efficacy of Laser Induced Breakdown Spectroscopy (LIBS) techniques in the field of nutritional science to detect essential as well as toxic metals exist in food stuff. With the increasing awareness of the effect of the elements present in food items on human health, the detection of essential as well as toxic metals in the trace level attracted more attention worldwide (DiSilvestro et al., 1998; Kannamkumarath et al., 2004). It is commonly recognized that dry fruits including nuts are a rich source of nutrients, mostly protein, vitamins, fat, minerals, as well as dietary fibers (Cardozo and Li, 1994). Dry fruits are good alternative to non-vegetarian food like meat and poultry with potential health benefits (Lino et al., 2002). Dry fruit helps to prevent many diseases such as ischemic heart diseases (I.H.D.), stroke by reducing the level of bad cholesterol (Sabaté, 1999). Some of the advantages of nutritional foods in case of diabetic patients include lower insulin requirements and better weight control (Segasothy and Phillips, 1999). Dry fruits taken in moderation provide important nutrients and maintain a balanced nutrition for human body. Also the nutritional density of the dry fruit, compared to fresh fruit is quite high as the nutrients are concentrated in solids after the water is removed. They are good sources of minerals, enzymes and vitamins, and they are easy to digest and fresh the blood and the digestive area (Sattar et al., 1989). Dry fruits have been part of essential human diet even in olden days taken from regular farming and wild fruit trees, as these are rich source of different nutrients (Dreher et al., 1996). Presence of certain essentials in our body act as catalysts in various metabolic activities (Mooradian and Morley, 1987; Samek et al., 1999). Elements in human body are present as a part of organic and inorganic compounds and the presence of hazardous metals results in disease and bad health. Also

the presence of both nutrient and toxins beyond certain limit in human body can cause bad effects, hence it is important to identify the abundance of essential and toxic elements in diverse food products that we use in our day to day life (Clemente, 1976). With the growing public health awareness, the revealing and quantification of nutrient and heavy metals exist in the food keeps the quality of food intake under check (Pfannhauser and Woidich, 1980). It has been reported that the storage pattern and bioavailability of these elements is sensitive to their chemical formulation (Vonderheide et al., 2002). Hence it is so crucial to disclose the elemental distribution in different segments and composition to furnish information on the toxicity/bioavailability of food based heavy metals (Fairweather-Tait, 1999).

This work gives emphasis on the detection of the most abundant and essential elements such as potassium (K) and magnesium (Mg) present in the food sample by LIBS detection technique and the outcomes were justified by means of inductively coupled plasma-atomic emission mass spectrometry (ICP-AES). Potassium is an important element that plays a role of keeping the level of sodium, the main contributor for the high blood pressure under check and relieves stress in blood vessel to lower the blood pressure. Magnesium is also an essential element for human metabolic processes, which include nucleic acids formation (DNA, RNA), protein separation, and production of cellular energy. Lower levels of magnesium are related to high levels of bad Low-density lipoprotein (LDL), which enhances the threat of heart attack and stroke. Moreover, magnesium is essential for the nervous system and efficient brain activity (Rosanoff, 2013). Besides beneficial nutritional elements, some hazardous species like Cu, Cr, as well as Pb exist in the dry fruit are also detected.

The chosen analytical procedure in the current work, LIBS, is basically an atomic emission spectroscopic technique, which has been proven to be quite reliable to reveal the chemical composition of the samples in solid liquid and gaseous phases (Hussain and Gondal, 2008; Gondal et al., 2009; Rehan et al., 2018d). When the high energy pulse of laser beam hits the sample surface, the generations of intense plasma take place through target heating, melting, and change of phase, ionization and excitation (Ali et al., 2016; Rehan et al., 2016, 2017, 2018b). LIBS method of detection is quite sensitive, rapid and does not require any sample preparation and hence a minute level of elements exist in the sample can easily be detected. The qualitative and quantitative study of various species exist in the samples was performed by studying the atomic emission lines and their intensities from the atomic elements present in the cooled plasma. The major advantage of LIBS technique over the other analytical methods is its capability to explore target in situ and distantly. Other well-known conventional diagnostic tools for elemental investigation are Inductively Coupled Plasma-Mass Spectroscopy (ICP-MS), Mass Spectroscopy (MS), Atomic Absorption Spectroscopy (AAS) and Flame Photometry (FP) (Kannamkumarath et al., 2004; Mutalik et al., 2011; Deeba et al., 2013). Still, those techniques usually involve a sequence of pre- treatment measures of sample which may be costly as well as time taking. For comparison purposes, here the results acquired by LIBS were also re-confirmed by standard ICP/AES methods.

2. Methods and material

2.1. LIBS set up

The graphic of LIBS system employed in the current work is similar as used previous (Rehan et al., 2018a,b,c,d,e,f) and is depicted as in Fig. 1. In short, the source of energy was the 1064-nm (fundamental) beam of laser from the pulsed Nd-YAG laser (Quantel Brilliant), of 5 ns pulse width, a 10 Hz pulse repetition rate having the ability to deliver the maximum laser pulsed energy of ≈ 400 mJ pulse^{-1}. The beam of laser was directed and focused on the surface of sample using a focusing lens of 20 cm focal length. The target was placed on a rotating mount to avoid the creation of crater which would alter the focal point of the lens and consequently the LIBS intensity. The sample was positioned at an optimized distance to avoid air breakdown in front of target.

The plasma emissions from sample surface was collected by a camera kept perpendicular to the laser beam and the collected light is fed into the input ports of the dedicated spectrometer (LIBS2000+, Ocean Optics Inc.) equipped with a CCD camera. The LIBS2000 + detector used five high resolution (HR) spectrometers having diverse grooves density on the grating (1800 lines/mm and 2400 lines/mm) to cover-up the spectral range from 200 nm to 700 nm. Every spectrometer has 2048-element linear CCD arrays with an optical resolution of ≈ 0.06-nm having the ability to work at dissimilar time delays.

2.2. Samples preparation for LIBS and ICP/AES investigation

Five different dried fruits available in the local markets in Pakistan were procured and the choice of dried fruits was based on their consumption and their availability. The dry fruit samples used for this study are Almonds (**Prunus dulcis**), Pistachio (**Pistacia vera**), Cashew (**Anacardium occidentale**), Black walnut (**Juglans nigra**), and White walnut (**Juglans cinerea**). First, all of the selected dried fruit samples were carefully washed in running water to remove dust and adhered particles (see Fig. 2). The washed samples were later rinsed with de-ionized water and subsequently dried in oven at ~55–80 °C. The desiccated samples were compressed to excellent powder. The pallets of 2-cm diameter and 2-mm thickness of these dry fruit samples were made using a hydraulic press by taking adequate amount of powdered samples, which provides a fairly flat surface to reduce signal fluctuation.

For ICP/AES, analysis the sample was prepared by typical working process (TWP) to digest and investigate. An amount of about 0.01-gram target was supplemented to ≈ 5-mL of HNO$_3$ (99-% pure-Fisher Scientific) and warmed up at ~60 °C till the volume of HNO$_3$ is reduced to 2-mL. Then the solution was cooled down for further dissolution in 40-mL of HNO$_3$ and reheated at ≈ 45 °C for ~2-hr to proper digest the dry fruit samples. The cool downed solution was then filtered using filter paper to eliminate undissolved traces. The resulting solution was used as sample for ICP spectrometry (Optima 2100-DV; Dual View-PerkinElmer).

3. Results

3.1. Verification of local thermodynamic equilibrium (LTE) from plasma temperature and (T_e) and electron number density (N_e)

The establishment of local thermo dynamical equilibrium in the laser generated plasma was justified using the parameters like the temperature of the plasma and density of electrons in the plasma and applying McWhirter criterion. The value of T_e is estimated using a linear plot of the Boltzmann distribution for a set of atomic emission lines. Also the stark widening peak shape of an isolated transition of a specific specie is used to calculate the electron number density (Rehan et al., 2018c). To estimate the electron temperature, the subsequent relation was employed.

$$ln\left(\frac{I_{ki}\lambda_{ki}}{A_{ki}g_k}\right) = ln\left(\frac{N(T_e)}{Z(T_e)}\right) - \frac{E_k}{kT_e} \qquad (1)$$

where, I_{ki} stand for intensity of transition between the higher level (k) and lower energy level (i), λ_{ki} stands for transition wavelength, A_{ki} provides the transition probability, g_k stands for statistical
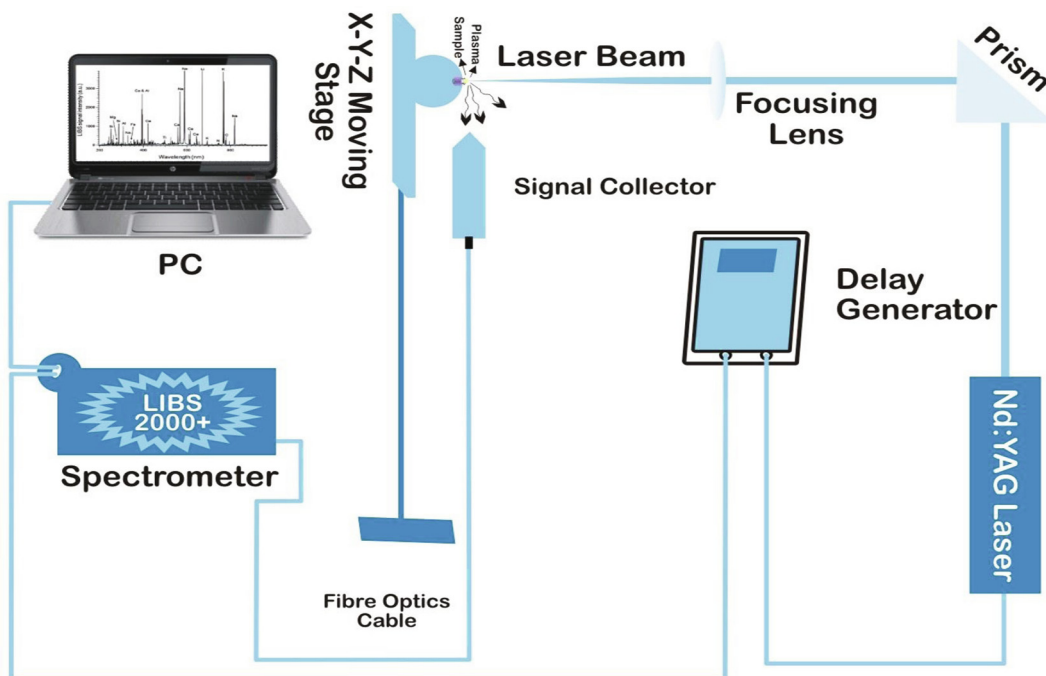
Fig. 1. Schematic of the LIBS setup for analysis of dry fruits samples.

Fig. 2. The collected dry fruit samples used in the present study.

The electron temperature was measured for all the samples within uncertainty of ~±10%, which basically occurs because of uncertainties in measurement of peak intensity, uncertainty in transition probabilities as well as in the fitting method as well. All of the spectroscopic data for transitions used to approximate the plasma temperature were acquired from NIST atomic database.

The value of N_e was measured from the full width half maximum (F.W.H.M.) of the Stark widening shape of a well isolated spectral emission line using relation as below:

$$\Delta\lambda_{1/2} = 2\omega\left(\frac{N_e}{10^{16}}\right) + 3.5A\left(\frac{N_e}{10^{16}}\right)^{\frac{1}{4}}\left[1 - \frac{3}{4}N_D^{-\frac{1}{3}}\right]\omega(\frac{N_e}{10^{16}}) \tag{2}$$

where $\Delta\lambda_{1/2}$ is the F.W.H.M. obtained using Lorentzian fitting of a stark widening line shape profile (nm), ω stands for electron impact width parameter which is a feeble dependent upon temperature (nm) (Tognoni et al., 2007), A is the ion broadening factor, N_e stands for electron number density (cm^{-3}), the factor 'A' gives the ion broadening parameter, whereas N_D is the number of species in the Debye sphere.

In Eq. (2), the first term on the right hand side shows the widening due to the contribution of electron, whilst the second term gives the impact of broadening due ion. In general, the involvement of broadening due to ions is incredibly minute consequently, it can be disregarded then Eq. (2) reduces to (Rehan et al., 2018e).

$$\Delta\lambda_{1/2} = 2w\left[\frac{N_e}{10^{16}}\right] \tag{3}$$

The Lorentzian fitting of experimentally observed line shape of Mg I at 285.2 nm (seen Fig. 3 (b)) gives the FWHM of ~0.1042 nm, thereby providing the analogous electron number density to be ~1.5 * 10^{17} cm^{-3}. The reason of selection of the spectral line Mg I at 285.2 nm was owing to the fact that this peak is well separated from another emission peaks. Since the two crucial plasma parameters are now determined i.e. T_e, and N_e, so we are now in the position to check whether our laser produced plasma is in L.T. equilibrium state, by McWhirter condition shown beneath (Rehan et al., 2018a):

weight of higher level (k), $N(T_e)$ is the population of upper-level, $Z(T_e)$ is the partition function, E_k gives the upper level's energy, k stands for the Boltzmann constant and T_e is the electron temperature.

By plotting the left hand side of Eq. (1) versus E_k, we obtained a straight line having the slope of $-1/kT_e$. Four neutral emission peaks of magnesium (Mg) at (278.2, 291.5, 383.8 and 389.1) nm, were selected and used to draw the Boltzmann plot at $3p^2$ $^3P_1 \rightarrow 3s3p\ ^3P_2^0$, $3p3d\ ^1D_2^0 \rightarrow 3s3d\ ^1D_2$, $3s3d\ ^3D_3 \rightarrow 3s3p\ ^3P_2^0$, and $3p3d\ ^3D_2^0 \rightarrow 3p^2\ ^3P_1$ correspondingly as exposed in Fig. 3 (a, b). Fig. 3 (a) gives a plot of linear Boltzmann form where the value of electron temperature comes out as ~6738 K.

Fig. 4. Plot showing the dependence of Laser signal intensity of Ca I (422.6 nm) spectral line upon laser irradiance on surface of sample.
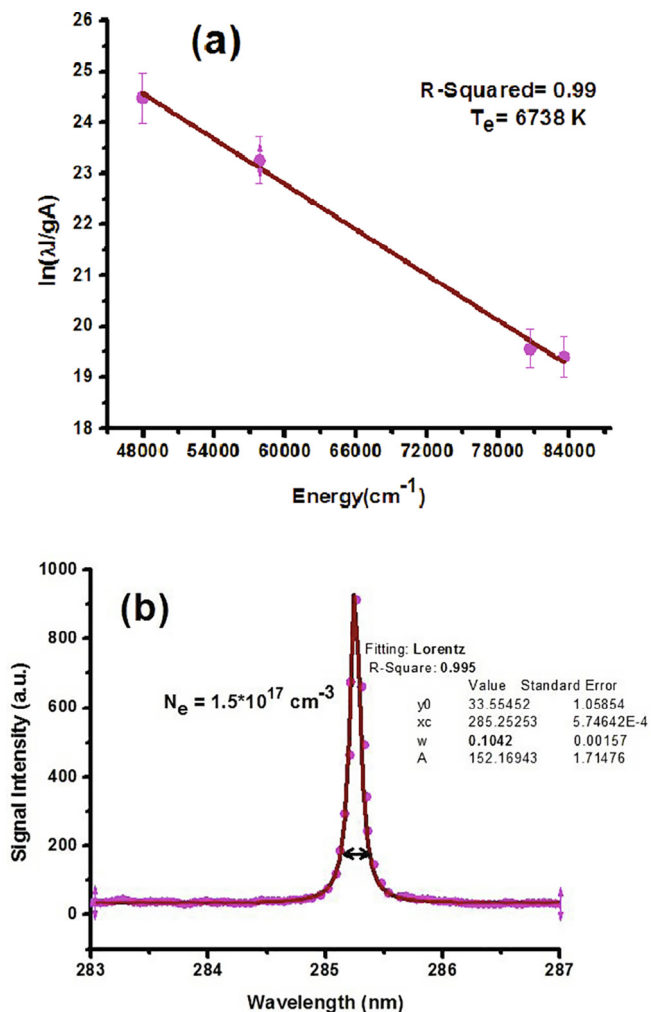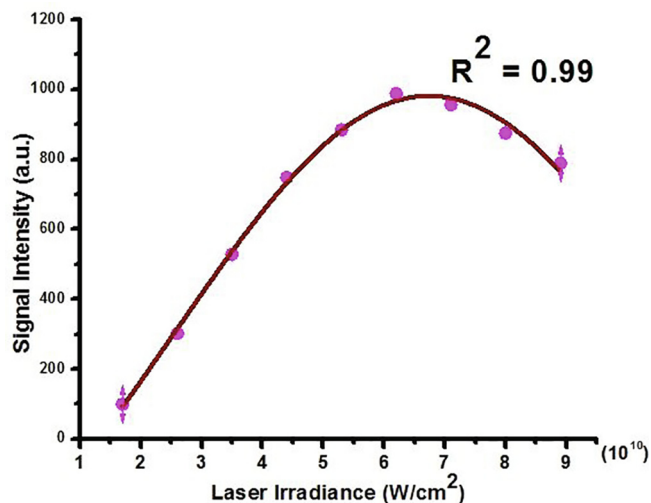
Fig. 3. (a, b). Typical plot of (a) Boltzmann using neutral magnesium emission lines of dry fruit's sample, (b) experimental fitting data of Mg-I at 285.2 nm to estimate of N_e.

$$N_e \geq 1.6 \times 10^{12} T_e^{\frac{1}{2}} (\Delta E)^3 cm^{-3} \tag{4}$$

where N_e (cm^{-3}) is the electron number density, T_e (K) is the electron temperature, and ΔE (eV) is the gape in energy between the greater and inferior state of transition under test. The expected critical electron number density comes out to be ~1.05 * E^{16} cm^{-3}, and was much less than the N_e calculated experimentally, hence the laser induced plasma fulfilled the necessary condition for LTE in our experiments.

3.2. Setting of optimized LIBS experimental parameters

There are two central experimental factors which are crucial in LIBS for its accuracy and also for its quantification of results: (i) optimum laser pulsed energy and (ii) the delay time between the laser excitement and the data acquisition. In the case of laser energy, initially the LIBS intensity increases with the laser pulse energy and this is because more laser intensity causes more excitation. However, this consequence stops at particular laser energy due to the formation of thick plasma owing to excessive laser energy and the plasma reabsorbed the emitted peaks. Hence optimum laser pulse energy has to be identified. As it is can be revealed in Fig. 4 that the LIBS intensity raises linearly with the laser irradiance until a peak laser irradiance of ~6.2 × 10^{10} W/cm^2, and subsequently falls down with the further increase of irradiance. Hence

for the optimum performance, the laser irradiance was kept at 6.2 × 10^{10} W/cm^2 throughout the experiment.

The second parameter that needs to be improved is the delay time between the laser excitation and the data achievement. The time we accumulate the atomic florescence after the excitation is very important to get a spectra that reflects the emission characteristics of the elements present in the sample plasma. Initially, the plasma is too hot with lots of ions and neutral entities and the collection of emitted (flourosecence) light at this phase will lead to a featureless continuum emission. On the another side collecting the fluorescence at very delayed time will lead to very low fluorescence owing to the full decay of the neutral fluorescence. Hence there exists an optimum time delay between the laser excitement and the atomic fluorescence gathering, where the resulting spectrum represents the elemental composition of the sample with optimum emission intensity. As far our case is concerned, the optimal delay time was identified by repeating the scan by changing the time delay between 0.5 μs to 3.5 μs, with an increment of 0.5 μs and the gate delay of 3.0 μs was observed incredibly appropriate for the gaining of fine LIBS spectra with a smaller amount background. The optimal value of gate delay was then applied during the current experimental steps.

In addition to the above two experimental parameters, the spacing between the focusing lens and sample was improved via observing the effect of lens to target distancing on the characteristic of spectra. To study the influence of spacing between lens and sample on integrated emission intensity, variable distances of (16, 17, 18, 19, 20, 21, 22, and 23) cm were selected. It was observed that as the targets were located at focal separation of focusing lens, the acquired peak intensities of the emitting particles were robustly fluctuating, signifying unsteady plasma. The finest agreement was found to be when the sample was located at $d < f$ (d = 19 cm) the spectral peaks attained were of stable heights.

4. Discussion

4.1. LIBS elemental detection in dry fruit samples

Having established and verified the local thermo dynamical equilibrium and also having established the optimum experimental conditions such as delay time, distance of lens from target and the laser irradiance, the system is expected to render a reliable qualitative and quantitative elemental study. Fig. 5 (a-d) show the LIBS spectra of dry fruit (pistachio sample) acquired in the
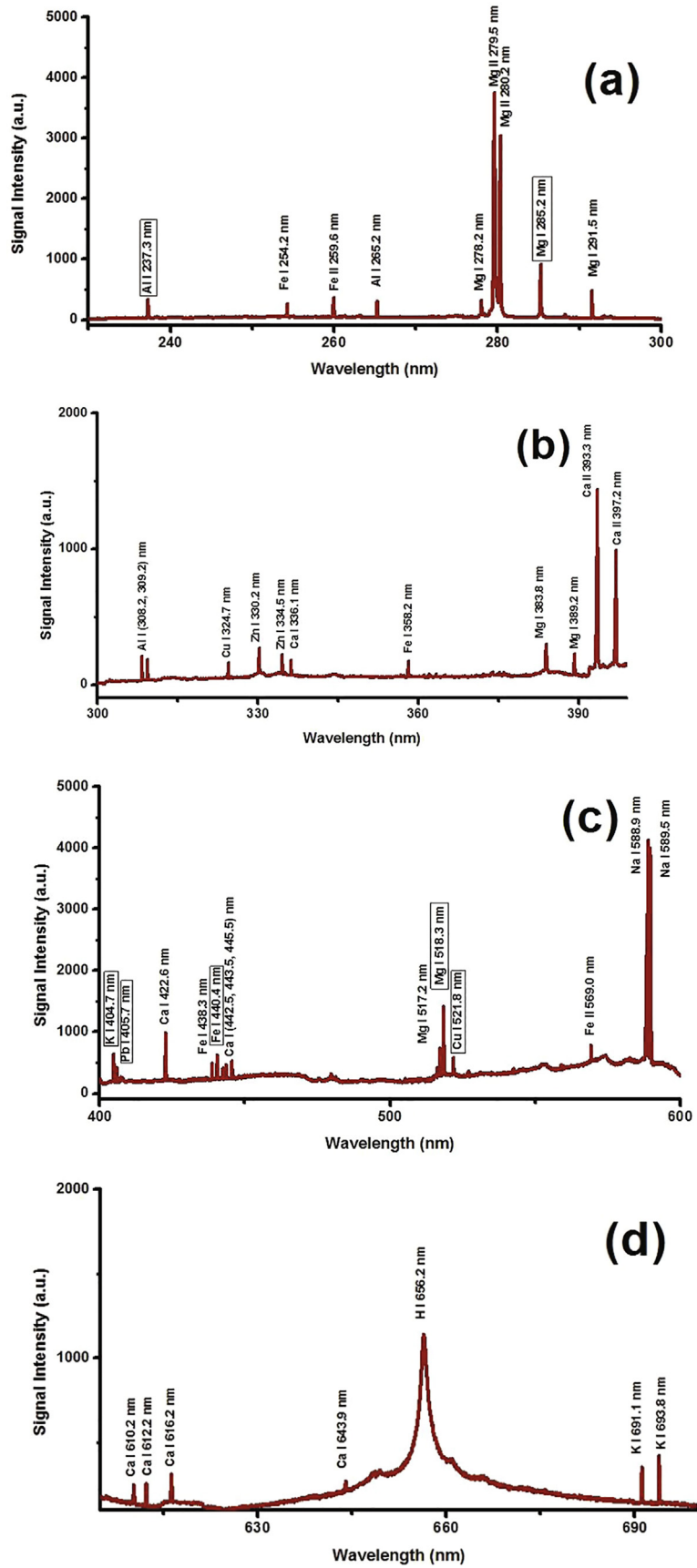
Fig. 5. (a-d). Characteristic LIBS spectrum for pistachio showing different elements detected on gated delay t_d of 3.0 μs also laser irradiance of 6.2×10^{10} W/cm^2.

Table 1
Quantification of essential and heavy metals in various dry fruit samples via LIBS and ICP-AES approaches.

Elements in dry fruit samples	Wavelengths (nm)	Assignment of optical transition	Samples	Concentration of LIBS and ICP-AES		Relative Accuracy (R. A.)	Standard-deviation (S.D.) LIBS
				LIBS (mg L^{-1})	ICP-AES (mg L^{-1})		
Al	237.3	$3s^2 4d\ ^2D_{5/2} \rightarrow 3s^2 3p\ 2P°_{3/2}$	Pistachio	35	30	0.207	1.09
			Almonds	39	35	0.156	1.05
			Black Walnut	33	28	0.180	1.00
			White Walnut	44	39	0.160	1.03
			Cashew	30	25	0.240	1.06
Ca	616.2	$3p^6 4s^5\ ^3S_1 \rightarrow 3p^6 4s4p\ ^3P°_2$	Pistachio	513	504	0.200	0.95
			Almonds	1397	1386	0.196	0.97
			Black Walnut	1114	1101	0.198	0.96
			White Walnut	1288	1275	0.207	1.00
			Cashew	2123	2111	0.167	0.99
Cr	425.4	$3d^5(^6S)4p^7P^0_4 \rightarrow 3d^5(^6S)4s\ ^7S_3$	Pistachio	ND	ND	N.D	N.D
			Almonds	4.9	5.5	0.198	0.71
			Black Walnut	3.5	4.0	0.192	0.67
			White Walnut	ND	ND	N.D	N.D
			Cashew	ND	ND	N.D	N.D
Cu	521.8	$3d^{10}4d^2D_{5/2} \rightarrow 3d^{10}4p\ ^2P°_{3/2}$	Pistachio	26	22	0.187	1.57
			Almonds	12	10	0.320	1.59
			Black Walnut	19	16	0.303	1.52
			White Walnut	17	14	0.260	1.55
			Cashew	16	140	0.334	1.58
Fe	440.4	$3d^7(4F)4p\ 3d^7(4F)^4p_4 \rightarrow 3d7(4F)4sa\ 3F$	Pistachio	282	277	0.309	1.60
			Almonds	142	137	0.328	1.62
			Black Walnut	131	126	0.338	1.66
			White Walnut	55	49	0.328	1.67
			Cashew	621	616	0.308	1.65
K	404.7	$3p^6 5p\ ^2P°_{1/2} \rightarrow 3p^6 4s\ ^2S_{1/2}$	Pistachio	6952	6937	0.316	1.75
			Almonds	3642	3629	0.325	1.79
			Black Walnut	1960	1946	0.327	1.78
			White Walnut	2173	2161	0.317	1.73
			Cashew	4445	4435	0.319	1.76
Mg	518.3	$3s^4 s3s\ ^4s_1 \rightarrow 3s^3 p\ 3\ s\ ^3p_2$	Pistachio	2235	2220	0.267	1.45
			Almonds	1411	1430	0.266	1.41
			Black Walnut	1421	1417	0.274	1.47
			White Walnut	1313	1325	0.268	1.44
			Cashew	2317	2304	0.272	1.48
Na	588.9	$2p^6 3p\ ^2P°_{3/2} \rightarrow 2p^6 3s\ ^2S_{1/2}$	Pistachio	65	59	0.281	1.16
			Almonds	125	117	0.245	1.11
			Black Walnut	29	25	0.376	1.10
			White Walnut	23	19	0.391	1.13
			Cashew	39	34	0.331	1.15
Pb	405.7	$6s^2 6p7s \rightarrow 6s^2 6p^2$	Pistachio	5	4.1	ND	0.55
			Almonds	ND	ND	ND	ND
			Black Walnut	ND	ND	ND	ND
			White Walnut	ND	ND	ND	ND
			Cashew	ND	ND	ND	ND
Zn	330.2	$3d^{10}4s\ ^4d_2 \rightarrow 3d^{10}4s4p\ ^3P°_1$	Pistachio	50	46	0.277	1.36
			Almonds	28	35	0.296	1.30
			Black Walnut	36	30	0.356	1.35
			White Walnut	38	30	0.303	1.33
			Cashew	50	46	0.274	1.34

ND = Not Detected.

spectral region of 230–700 nm, split into four spectral segments and the spectra in Fig. 5 (a-d) show the recognition of the species exist in the target. Here only representative spectrum of pistachio sample was shown for the sake of time and space. The LIBS spectra were acquired at a gate delay at 3 μs, laser irradiance of ∼6.2 × 10^{10} W/cm^2, lens to target distance at 19 cm, which are the optimized parameters discussed in the preceding section. The optical fiber was positioned an optimum value of 10 mm from the plasma.

The elements in the LIBS spectra were identified by NIST atomic database. This elemental identification and quantification is possible because of the achievement of local thermo dynamical equilibrium where the self-absorption of the neutral peaks by plasma

itself is drastically reduced and also because the lines are free from the continuum background and are well resolved due to the proper selection of experimental parameters. LIBS spectra were recorded for all the dry fruit samples selected for this study and it was found that the emission mostly takes place mainly from the neutral species with only a few emissions from the singly charged ions (II). It was also found that in terms of the presence of nutritional elements, all the dry fruits show no significant qualitative variation, and their difference lies in the quantitative variations among the different dry fruit samples (see Table 1). However, in the case of undesired toxic elements the dry fruits differ as explained below. The LIBS emission spectra of all the dry fruit under test showed the presence of essential species such as atomic K (404.7 nm, 691.1 nm, and 693.8 nm), atomic as well as singly ionized Ca-I (336.1 nm, 422.6 nm, 442.5 nm, 443.5, 445.4 nm, 610.2 nm, 612.2 nm, 616.2 nm, 643.9 nm), Ca II (393.3 nm, 397.3 nm), atomic and singly ionized lines of Mg-I (I 278.2 nm, 285.2 nm, 291.5 nm, 383.8 nm, 389.1 nm, 517.2 nm, 518.3 nm), Mg II (279.7 nm, 280.2 nm), neutral Fe (254.2 nm, 358.2 nm, 438.3 nm, 440.4 nm, 538.3 nm), Fe II (259.6 nm, 569.0 nm), strong atomic Zn (330.2 nm, 334.5 nm), as well as atomic Aluminum (237.2 nm, 265.2 nm, 308.2 nm, and 309.3 nm). The resonance peaks of Na (588.9 nm, 589.5 nm) were observed as well. The toxin Cu I at $3d^{10}4d\ ^2D_{3/2} \rightarrow 3d^{10}4p\ 2P^0_{3/2}$ was identified in all the studied dry fruit samples, whereas marker peaks of heavy Pb I at $6p_{1/2}6p_{3/2} \rightarrow 6p_{1/2}7s_{1/2}$, was noticed just in pistachio. Strong atomic line of Chromium at $3d^5(^6S)\ 4p\ ^7P^0_4 \rightarrow 3d^5(^6S)\ 4s\ ^7S_3$ was observed in almonds and black walnut only. The presence of nutritional elements in the dry fruit sample is such that all the dry fruit samples under study were found to be much rich of K followed by Mg. The emission peaks of potassium are feeble across the present wavelength region because the resonance lines of K are between 766 and 770 nm, which lies out of the spectral region of our spectrometer. The LIBS spectra in Fig. 5 (a-d) show the existence of H_α at 656.2 nm ($3p\ ^2P^0_{3/2} \rightarrow 2\ s\ ^2S_{1/2}$), which emerge from the atmosphere as the dry fruit plasma was formed in ambient environment. Other powerful atmospheric peaks of N and O (about 744-nm and 777-nm) were not observed as they were beyond the enclosed wavelength region of our spectrometer. The selected wavelengths (as mentioned in Table 1) for every constituent were chosen for both qualitative as well as quantitative investigation.

For the analytical measurements of the elements exist in the selected targets, the particular standard calibration curves were drawn by spiking up the sample matrix with known concentrations of a particular element and recording the corresponding LIBS intensity. The abundance of a specific species in the typical reference samples and their relevant LIBS signal samples provides a relationship linking the integrated signal strength and the anonymous abundance of essentials.

$$I = \left(\frac{h\nu_{ji}NA_{ji}g_{ji}}{Q}\right)e^{\left(-E_j/kT\right)} \qquad (5)$$

The Eq. (5) can be used to estimate the population density 'N' of a neutral or ionized species energized from level i (ground) to level j (upper) and is relative to the rate of mass of ablated matter and energy of focused laser pulse as can be seen in Fig. 4. For every element, their particular marker wavelength (specified in Fig. 4) were chosen for the plotting of a calibration curve. The typical samples were arranged by the addition of known amounts of elements in the sample (target samples) matrix. The calibration standard samples of different concentrations (5, 1000, 3000, 5000, 7000, and 9000 mg L^{-1}) (parts per million) of desired elements in target (dry fruits) matrix were arranged and LIBS spectra were acquired for such six abundances.

As an example, the calibration curves for Mg and Fe using that atomic transition line at 518.3 nm and 440.4 nm for pistachio are depicted respectively in Fig. 6 a, and Fig. 6 b. From the calibration curves, the abundance of essential and heavy metals exists in the samples under test were evaluated and listed in Table 1. It is obvious from Table 1, that the abundance of K, and Mg were high in all the dry fruit samples under study which are important for health as stated in the previous sections.

From Table 1, it is clear that the quantity of essential metals like K, and Mg varies from 1960 to 6952 mg L^{-1} and 1313–2317 mg L^{-1} respectively in various dry fruit samples. The concentrations of K and Mg for various dry fruit sample are presented in Fig. 7 a, where it is quite clear that the highest level of K is present in pistachio and the lowest levels of K is found in black walnut. Potassium is a momentous mineral that is essential for different metabolism in human body and it helps lowering blood pressure by balancing out the harmful effects of the table salt. The deficiency of potassium leads to the conditions like sleeplessness, constipation, depression and dysthymia. Critically small levels of potassium are known to result in serious health conditions like cardiac arrhythmia, and which makes it all the more imperative to maintain an eye for the level of potassium in the body (Krishna and Kapoor, 1991). From Fig. 7 b, it is clear that cashew has highest level of magnesium (2317 mg L^{-1}) followed by pistachio (2235 mg L^{-1}). Total cholesterol in human blood is mainly composed of low-density lipoprotein (LDL) as well as high-density lipoprotein (HDL) cholesterol, in which the elevated the level of
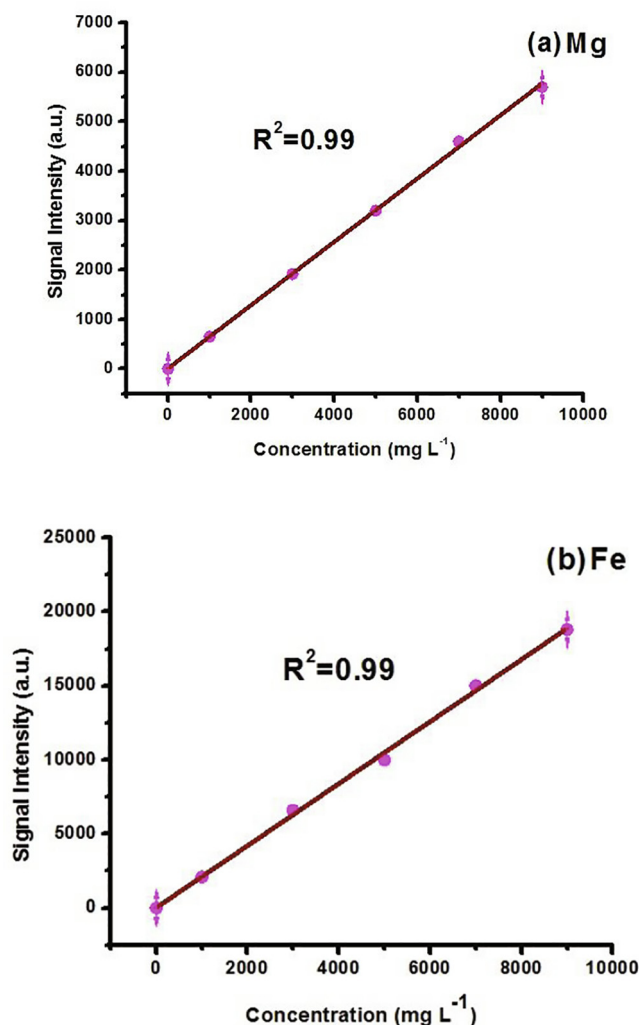

Fig. 6. (a, b). Representative standard calibration curves of (a) Mg (b) Fe in pistachio.
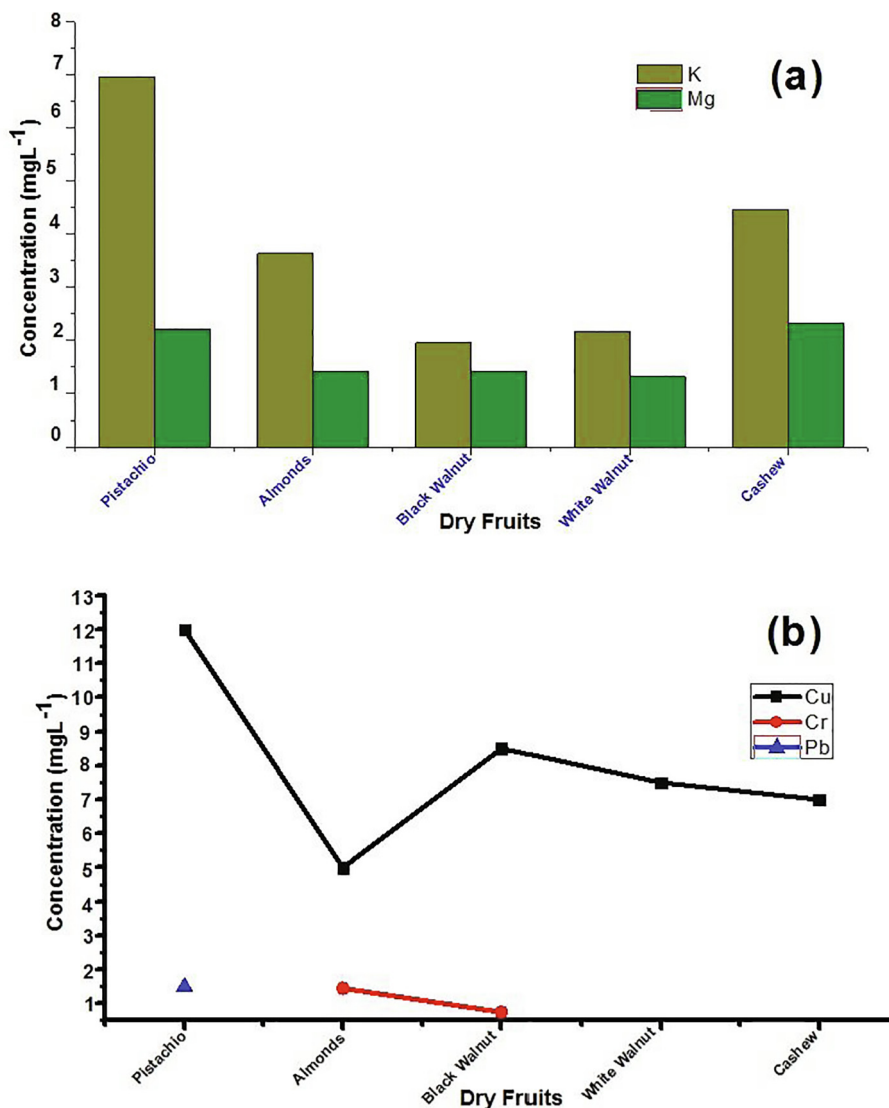
Fig. 7. (a, b). Concentration profile of (a) potassium and magnesium in different dry fruits, and (b) toxic metals in the studied dry fruit samples.

LDL raise the risks for heart disease and stroke in humans. Lower levels of magnesium are associated with high levels of Low-density lipoprotein (LDL) i.e. bad cholesterol.

The nutritional profile presented in terms of the elements presents in different dry fruit helps to deal with the common problem of under nutrition among the under privileged population of Pakistan. This will help to dispense right amount of potassium and magnesium, which are essential for the human metabolism. Our study shows that dry fruits especially pistachio is rich supply of potassium and can be taken as supplement to overcome potassium deficiency, moreover cashew was found to be highly rich of magnesium so its use is recommended to overcome excess of Low-density lipoprotein (LDL).

In addition to nutritional elements, our work was extended to study the presence of toxins like chromium (Cr), copper (Cu) and lead (Pb) in the studied dry fruit samples. It is clear from Table 1 and also Fig. 7 that Cu is found in all the dry fruit samples under study with concentrations ranging between 12 mg L^{-1} and 26 mg L^{-1}. The highest value for the concentration of copper was found in pistachio and lowest concentration was observed in almonds. Copper intake from peppers has no effect on health as it was noticed to be below the maximum permissible limit.

Also, Cr was identified only in almonds (4.9 mg L^{-1}) and black walnut (3.5 mg L^{-1}) whose amount was above the allowed boundary fixed by the Saudi Food and Drug Authority (SFDA) (see Fig. 7 b). The presence of chromium in plant based food basically stem from air water and soil and from the food intake it enters the human body and causes health dis orders related to vital organs like kidney, liver, and lung. Consequently, reliable information of the quantity of chromium present in dry fruits is very important to keep the intake of this harmful element under check. In the case of Pb, it was found only in pistachio with the concentration of 5.0 mg L^{-1} and is below the maximum permissible limit.

4.2. Validation of LIBS detection system

In order to validate the quantitative elemental analysis using LIBS results, the LIBS outcomes were compared with the standard ICP-AES measurements and it was observed that outcomes from both analytical methods are in good agreement. For this comparison, the relative accuracy (RA) as described in Eq. (6) and the relative standard deviation (RSD) as described in Eq. (7) are used.

$$R.A. = \frac{|d| + S.D. \times \frac{t_{0.975}}{\sqrt{n}}}{M} \qquad (6)$$

In Eq. (6) for relative accuracy, "d" gives the difference between the results of LIBS and the ICP (standard method). S.D. stands for the standard deviation of LIBS calculations; M gives the outcomes from standard approach, n gives the number of measurements and $t_{0.975}$ stands for the t value (at 2.5% error confidence). As can be seen from Table 1, the relative accuracy lies in the range of 0.1–0.3 which is pretty good enough for any excellent instrument. Moreover, the measurement of relative standard deviation (R.S.D.) was performed as,

$$R.S.D(\%) = \frac{standard deviation(\sigma_B)}{mean(n)} \tag{7}$$

The relative standard deviation was observed to reduce via the number of shots up to 25 shots but afar no enhancement in RSD was found. In our case the RSD value was found to be ~3.4%.

5. Conclusion

A laser induced breakdown spectrometer was optimized to analyze essential and heavy metals present in the dry fruits (Pistachio, Almonds, Black walnut, White walnut, and Cashew) available in Pakistani market were studied. Using our LIBS detection system, the nutritional elements such as Al, Mg, Ca, Fe, K, Zn, and Na and toxic elements such as Pb, Cr, Cu were detected in dry fruits. For a reliable elemental detection using LIBS techniques, the local thermo dynamical equilibrium of the laser induced plasma was established and verified using McWhirter criterion based on the electron number density in the plasma and the system was experimentally optimized by choosing appropriate laser fluence and the delay between the excitation of laser and the data attaining. Our study shows that the highest level of K is present in pistachio and the lowest levels of K is found in black walnut and also the cashew has highest level of magnesium followed by pistachio. In the case of toxic metals, Cu is found in all the dry fruit samples under study with concentrations ranging between 12 mg L^{-1} and 26 mg L^{-1}. The highest value concentration of copper was found in pistachio and lowest concentration was observed in almonds. Cr was identified only in almonds (4.9 mg L^{-1}) and black walnut (3.5 mg L^{-1}) and Pb was found only in pistachio with the concentration of 5.0 mg L^{-1} and is below the maximum permissible limit. The elemental analysis and the quantification of dry fruit was validated using standard inductively coupled plasma-atomic emission spectrometry (ICP-AES) and both the results are in superior conformity.

Declaration of Competing Interest

The authors declare that they have no known competing financial interests or personal relationships that could have appeared to influence the work reported in this paper.

Acknowledgement

References

Ali, A., Khan, M., Rehan, I., Rehan, K., Muhammad, R., 2016. Quantitative classification of quartz by laser induced breakdown spectroscopy in conjunction with discriminant function analysis. J. Spectrosc. 2016, 1–7.

Cardozo, M.S., Li, B.W., 1994. Total dietary fiber content of selected nuts by two enzymatic-gravimetric methods. J. Food Compost Anal. 7, 37–43.

Clemente, G., 1976. Trace element pathways from environment to man. J. Radioanal. Nucl. Chem. 32, 25–41.

Deeba, F., Abbas, N., Ahmed, R., 2013. Market basket survey of selected dry fruits as a potential source of potassium. Pak. J. Biochem. Mol. Biol. 46, 22–25.

DiSilvestro, R.A., O'Dell, B., Sunde, R., 1998. Handbook of nutritionally essential mineral elements. Free Radic. Biol. Med. 1998 (24), 684.

Dreher, M.L., Maher, C.V., Kearney, P., 1996. The traditional and emerging role of nuts in healthful diets. Nut. Revi. 54, 241–245.

Fairweather-Tait, S.J., 1999. The importance of trace element speciation in nutritional sciences. J. Anal. Chem. 363, 536–540.

Gondal, M.A., Nasr, M.M., Ahmed, Z., Yamani, Z.H., 2009. Determination of trace elements in volcanic rock samples collected from cenozoic lava eruption sites using LIBS. J. Environ. Sci. Heal. A. 44, 528–535.

Hussain, T., Gondal, M., 2008. Monitoring and assessment of toxic metals in Gulf War oil spill contaminated soil using laser-induced breakdown spectroscopy. Environ. Monit. Assess. 136, 391–399.

Kannamkumarath, S.S., Wuilloud, R.G., Caruso, J.A., 2004. Studies of various elements of nutritional and toxicological interest associated with different molecular weight fractions in Brazil nuts. J. Agric. Food Chem. 52, 5773–5780.

Krishna, G.G., Kapoor, S.C., 1991. Potassium depletion exacerbates essential hypertension. Annals. Int. Med. 115, 77–83.

Lino, M., Marcoe, K., Dinkins, J.M., Hiza, H., Anand, R., 2002. The role of nuts in a healthy diet. Fam. Econ. Rev. 14, 80–85.

Mooradian, A.D., Morley, J., 1987. Micronutrient status in diabetes mellitus. Am. J. Clin. Nutr. 45, 877–895.

Mutalik, V.K., Baragi, J.G., Mekali, S.B., Gouda, C.V., Vardhaman, N., 2011. Determination of estimation of potassium ion in dry fruits by flame photometry and their proximate analysis. J. Chem. Pharm. 3, 1097–1102.

Pfannhauser, W., Woidich, H., 1980. Source and distribution of heavy metals in food. Toxicol. Environ. Chem. 3, 131–144.

Rehan, I., Gondal, M., Rehan, K., 2018a. Determination of lead content in drilling fueled soil using laser induced spectral analysis and its cross validation using ICP/OES method. Talanta 182, 443–449.

Rehan, I., Gondal, M., Rehan, K., 2018b. Optimized laser-induced breakdown spectroscopy for determination of xenobiotic silver in monosodium glutamate and its verification using ICP-AES. Appl. Optics 57, 3191–3197.

Rehan, I., Khan, M., Muhammad, R., Khan, M., Hafeez, A., Nadeem, A., Rehan, K., 2018c. Operational and spectral characteristics of a Sr–Ne glow discharge plasma. Arab. J. Sci. Eng. 44, 561–568.

Rehan, I., Khan, M., Rehan, K., Abrar, S., Farooq, Z., Sultana, S., Saqib, N.U., Anwar, H., 2018d. Optimized laser-induced breakdown spectroscopy for the determination of high toxic lead in edible colors. Appl. Optics 57, 6033–6039.

Rehan, I., Khan, M.Z., Ali, I., Rehan, K., Sultana, S., Shah, S., 2018e. Spectroscopic analysis of high protein nigella seeds (Kalonji) using laser-induced breakdown spectroscopy and inductively coupled plasma/optical emission spectroscopy. App. Phy. B. 124, 1–8.

Rehan, I., Khan, M.Z., Rehan, K., Mateen, A., Farooque, M.A., Sultana, S., Farooq, Z., 2018f. Determination of toxic and essential metals in rock and sea salts using pulsed nanosecond laser-induced breakdown spectroscopy. Appl. Optics 57, 295–301.

Rehan, I., Rehan, K., Sultana, S., ul Haq, M.O., Niazi, M.Z.K., Muhammad, R., 2016. Spatial characterization of red and white skin potatoes using nano-second laser induced breakdown in air. EPJAP 73, 10701.

Rehan, K., Rehan, I., Sultana, S., Khan, M.Z., Farooq, Z., Mateen, A., Humayun, M., 2017. Determination of metals present in textile dyes using laser-induced breakdown spectroscopy and cross-validation using inductively coupled plasma/atomic emission spectroscopy. J. Spectros. 2017, 1–9.

Rosanoff, A., 2013. The high heart health value of drinking-water magnesium. Medical Hypo. 81, 1063–1065.

Sabaté, J., 1999. Nut consumption, vegetarian diets, ischemic heart disease risk, and all-cause mortality: evidence from epidemiologic studies. Am. J. Clin. Nutr. 70, 500s–503s.

Samek, O., Liska, M., Kaiser, J., Krzyzanek, V., Beddows, D.C., Belenkevitch, A., Morris, G.W., Telle, H.H., 1999. Laser ablation for mineral analysis in the human body: integration of LIFS with LIBS. Biomed. Sensors, Fibers, Opt. Delivery Systems. Proc. SPIE 3570, 263–272.

Sattar, A., Wahid, M., Durrani, S.K., 1989. Concentration of selected heavy metals in spices, dry fruits and plant nuts. Plant Foods Hum. Nutr. 39, 279–286.

Segasothy, M., Phillips, P.A., 1999. Vegetarian diet: panacea for modern lifestyle diseases?. QJM 92, 531–544.

Tognoni, E., Cristoforetti, G., Legnaioli, S., Palleschi, V., Salvetti, A., Müller, M., Panne, U., Gornushkin, I., 2007. A numerical study of expected accuracy and precision in calibration-free laser-induced breakdown spectroscopy in the assumption of ideal analytical plasma. Spectrochim. Acta B 62, 1287–1302.

Vonderheide, A.P., Wrobel, K., Kannamkumarath, S.S., B'Hymer, C., Montes-Bayón, M., Ponce de León, C., Caruso, J.A., 2002. Characterization of selenium species in brazil nuts by HPLC− ICP-MS and ES-MS. J. Agric. Food Chem. 50, 5722–5728.